Spacecraft Fire Safety Predictions using Validated Saffire Model

Justin Niehaus[1], David Urban[2], Gary Ruff[3], Gordon Berger[4] and John Easton[5]
NASA Glenn Research Center, Cleveland, OH 44135, USA

A model developed using Fire Dynamics Simulator (FDS) that aimed to determine the effect of a fire in a spacecraft was validated by data collected during the Saffire campaign. The model used inlet and outlet temperatures and CO_2 concentrations of the Saffire payload where fire spread was taking place to determine the amount of heat and combustion products that made it into Northrop Grumman's Cygnus vehicle. The model was then validated using six remote sensors in various places in the vehicle, as well as a far field device (FFD) in the open zenith section that was representative of average vehicle values. The current work focuses on using the model to predict fire safety scenarios. One simulation aimed to determine the fate of HCl, which sticks to surfaces. The model prediction showed that the HCl was removed from the atmosphere rapidly. This compared well against the FFD data in the Saffire VI campaign event where a bottle of 5% HCl was released into the vehicle. An additional simulation where the Environmental Control and Life Support System (ECLSS) was shut off once the FFD reached 5 ppm of HCl showed that HCl stayed in the atmosphere considerably longer. Continuing the simulation with the ECLSS activated and after temperatures returned to their initial conditions, resulted in a rapid removal of HCL similar to that observed in the original HCl release scenario model. Finally, a simulation that used the heat release rate from a lithium-ion battery test to determine the effect it would have on a spacecraft was performed. This simulation used a heat addition rate that is considerably higher than what was determined from the burning of solid fuels in the Saffire campaign and hence produced a non-trivial temperature increase in more locations within the vehicle.

Nomenclature

C_p	=	specific heat
ECLSS	=	Environmental Control and Life Support System
FDS	=	Fire Dynamics Simulator
FFD	=	Far Field Diagnostics
HAR	=	Heat Addition Rate
HEPA	=	High-Efficiency Particulate Air
ISS	=	International Space Station
k	=	conductive heat transfer coefficient
LIB	=	Lithium Ion Battery
lpm	=	liters per minute
MFC	=	Mass Flow Controller
MGR	=	Mass Generation Rate
NG	=	Northrop Grumman
NIST	=	National Institute of Standards and Technology
PMMA	=	Polymethyl Methacrylate
ppm	=	parts per million
psig	=	pounds per square inch gauge
RS	=	Remote Sensor

[1] Aerospace Engineer, Low-Gravity Exploration Technology Branch, 21000 Brookpark Road, Cleveland, OH 44135.
[2] Supervisor Aerospace Engineer, Low-Gravity Exploration Technology Branch, 21000 Brookpark Road, Cleveland, OH 44135.
[3] Fire Safety Subject Matter Expert, NASA NESC, Langley, VA 23681.
[4] Scientist, E Street Technologies, 21000 Brookpark Rd., MS 77-5, Cleveland, OH 44135
[5] Associate Staff Scientist, Case Western Reserve University, 21000 Brookpark Rd., MS 77-5, Cleveland, OH 44135

SFU = Saffire Flow Unit
SIBAL = Solid Inflammatory Boundary at Low-Speed fabric
SMAC = Spacecraft Maximum Allowable Concentration
α = thermal diffusivity
ρ = density

I. Introduction

Planning effective responses to a fire on a spacecraft is one of the most impactful ways to reduce the risk to a spacecraft's mission success and crew safety. Oxygen levels for planned missions will be elevated, only adding to this risk [1-3]. Increased oxygen reduces prebreathe time requirements and complexity for EVA operations, as well as decreases mass required for structural containment due to smaller pressure differentials between cabin and the vacuum of space [3]. Full-scale testing at the planned atmosphere, as implemented in previous space programs [4-6], are a way of quantifying the increased risk. This type of fire data was collected during the Saffire project in a microgravity environment [7-9]. Over six sets of orbital experiments, the Saffire payload burned thermally thick polymethyl methacrylate (PMMA) and thin (cotton or solid inflammatory boundary at low-speed fabric (SIBAL)) fuels on Northrop Grumman's (NG) Cygnus vehicle to study flame spread and fire effects on a space craft in a microgravity environment. These were carried out after Cygnus undocked from a resupply mission to the International Space Station (ISS).

A computational model of Saffire VI was previously developed and validated against six remote sensors (RS) in Cygnus that measured temperature and CO_2 during burn events in the Saffire campaign [10-13]. The model used the CO_2 response or the six RS to validate that the trash and cargo placement in the model provided the appropriate flow paths, as well as the free volume matched the experimental value. The temperature response of the RS closest to the Saffire payload was used to calibrate an effective heat transfer coefficient of the cargo, and validate it against the other RS. The work described in this paper uses the validated computational model to predict other spacecraft fire scenarios not produced in the Saffire experiments. The first scenario being set of simulations explored acid gas transport with the objective of determining the effect flow had on the fate of acid gas in a spacecraft. The second set of simulations involved using experimental data from a lithium-ion battery (LIB) fire, an increasingly relevant fire hazard, with the objective of simulating a more energetic fire than what was provided by the Saffire burn event.

A fire in a spacecraft can create acid gases such as HCl from the burning of electronics, which stick to surfaces unlike other combustion products. In addition to the burn events in the Saffire VI experiments, a bottle of HCl was released to study the fate of acid gas in a spacecraft. While not measured at the RS locations, it was measured at the Far Field Device (FFD) in the zenith section of the cabin, which was representative of average cabin values. To complement the microgravity tests, small-scale ground testing was performed to determine the uptake of acid gas by typical spacecraft materials, predominantly treated aluminum [14,15]. This uptake rate was applied to the surfaces of the Saffire model and the transport to the FFD in the model was compared to the experiment. Once a reasonable comparison was observed, additional simulations were performed with the objective to determine the effect on cabin flow on the fate of acid gas. A typical recommendation during a fire in spacecraft is to turn off the flow to prohibit oxygen transport to the flame to encourage extinction [5, 16]. Simulations were run where once HCl reached a threshold value, the environmental control and life support system (ECLSS) flow, as well as any flow associated with the Saffire Flow Unit (SFU) were shut off to see the effect on the fate of HCl. An additional simulation was run where the flow was turned back on once the temperature returned to the initial value.

The last set simulation used the heat addition rate (HAR) produced from lithium-ion battery (LIB) tests with the objective of predicting a relevant fire hazard and a more energetic fire than that produced by the burning of SIBAL or PMMA would have on a spacecraft. The heat released into Cygnus from the burn events of Saffire proved to not increase the temperature in the vehicle significantly. The ground tests involving LIB fires provided a larger max HAR and more overall heat than the Saffire burn events, and hence a hotter cabin.

II. Experiments

A. Saffire Microgravity Experiments

The Saffire campaign of experiments performed large-scale burn events to study the smoke plume and combustion product transport within an orbiting vehicle [7-9]. All six of these set of experiments took place in between separate resupply missions to the ISS and controlled burn up in the atmosphere, giving approximately three days of microgravity combustion experimentation and data downlink. Saffire VI, which is the focus of this paper, took place in December of 2023. The pressure vessel, which is approximately 3 meters in diameter by 4 meters in length, also contained the environmental control and life support system (ECLSS) for maintaining flow conditions, and various instrumentation for measuring temperature and combustion product concentrations throughout the vehicle. Figure 1 gives a schematic of the Cygnus vehicle and Saffire experiments.

Cargo and trash were placed in Cygnus to create channels to transport heat and combustion products from the outlet of Saffire in the nadir section to the zenith section of the spacecraft. This created four different channels, similar to the forward port standoff illustrated in Figure 1. Each channel had an RS that measured temperature and combustion products, such as CO_2. In order to apply heat and combustion products into the domain, or the gas volume of the model, a HAR and a mass generation rate (MGR) are applied to the 50 cm^2 SFU outlet that flows hot air into the Cygnus vehicle.

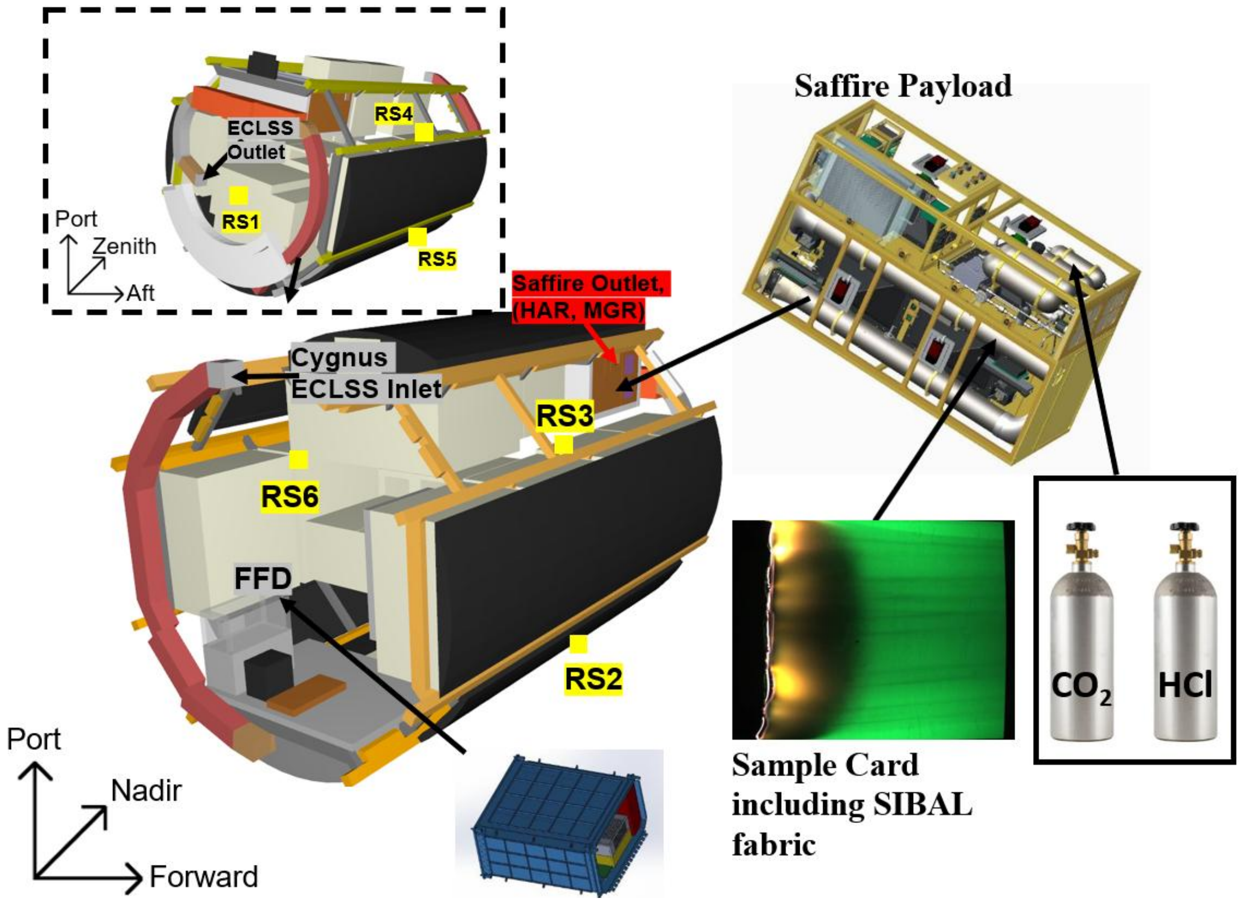

Figure 1. Saffire VI experimental schematic. *Dashed box area represents the Cygnus vehicle from the Nadir side for a view of the ECLSS outlet, RS1 and RS4 in the Aft Port standoff. Foam is removed in the Forward Port and Aft Port standoffs for visualization purposes. RS2 and RS5 are shown outside the foam for visualization purposes.*

Nine experimental events took place during the Saffire VI campaign, including four attempted burn events, two flow visualization tests, a gas release event, and two CO_2 scrubs. The initial atmospheric conditions used in the model were the same used during the SIBAL burn of Saffire VI: 54.1 kPA, 31.0% oxygen, and a temperature of 24.3°C. More details of the experiment can be found in previous work [7-9].

B. HCl Ground Testing

Experiments to characterize the uptake of acid gas onto surfaces have taken place to support the Saffire project and help determine the fate of acid gases after a spacecraft fire. Specifically, HCl uptake onto treated aluminum surfaces has been measured in past studies [14, 15]. Figure 2 gives a schematic of the experimental setup. A bottle of dry air and a bottle of approximately 50 parts per million (ppm) of HCl balanced with nitrogen were used to flow a

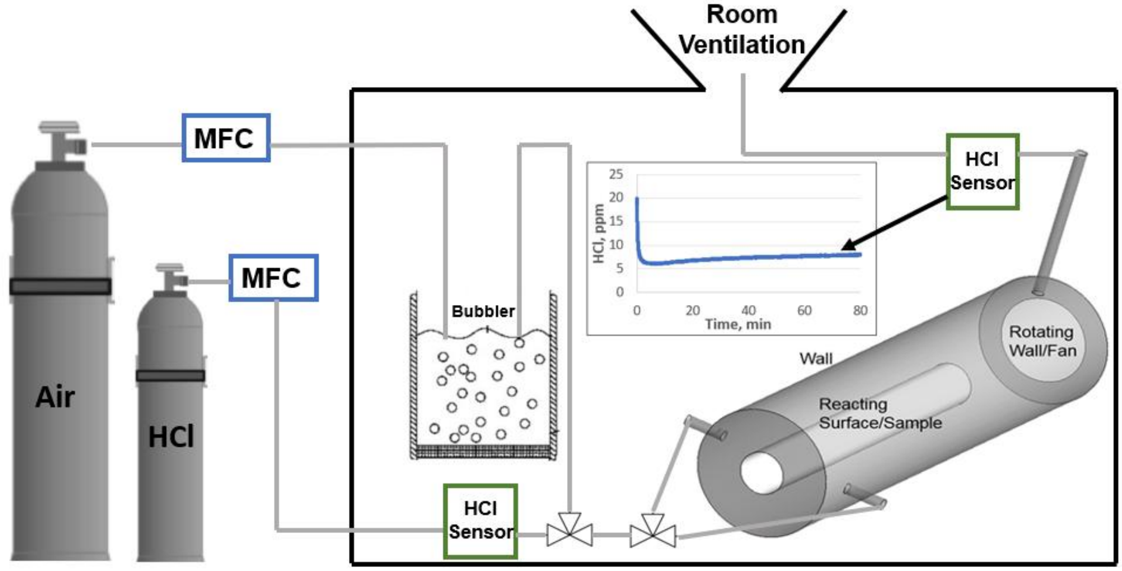

Figure 2. Acid gas experimental schematic and results.

gas stream through a cast acrylic test cell until it was saturated by HCl. An aluminum rod would then be inserted into the test cell, decreasing the response of the outlet HCl sensor. The air stream could be passed through a bubbler to control the humidity of the air stream.

In mostly dry flow conditions, there is a finite capacity of aluminum to uptake HCl [14]. In the presence of the type of humidity you would find in a comfortable room or spacecraft (40-60% humidity at approximately 20 °C), there is a near infinite capacity to uptake HCl. The graph in Figure 2 shows a typical response of the outlet HCl sensor when flowing 2 liters per minute (lpm) of HCl into the reactor and 2 lpm of air through the bubbler, providing a humidity of approximately 50%, [17]. The difference between the inlet and outlet sensor was used to determine the rate of uptake by the sample inserted into the reactor. This rate of HCl uptake was applied to the cargo in the Saffire model. More information on the experimental setup and previous results can be found in earlier research [14, 17]. Saffire VI flew 1-liter HCl bottles at 100 pounds per square inch gauge (psig) pressure and 5% concentration balanced with N_2 producing a total HCl of 0.59 g which was released from the bottle in the SFU at a rate of 2.68×10^{-3} kg-HCl/m^2-s.

C. Lithium-Ion Battery Ground Testing

An experiment was set up to determine the heat and product release of a LIB cell pack during thermal runaway. The apparatus included an outer enclosure that was connected to room ventilation air flow 2.29 m tall by 2.44 m in width and depth. Inside the outer enclosure was an inner enclosure where the battery cell pack was ignited with two hot plates. The inner enclosure connected to a measurement duct that was 76 mm in diameter and probed the air stream for O_2, CO_2, CO concentration and temperature. Figure 3 shows a schematic of the experimental apparatus.

The data used to provide the HAR for the Saffire model was collected from the burning of a 97 Watt-hour, 6 LIB cell pack. The batteries were at their fully charged state. The cells were ignited with two 500 W strip heaters, each igniting three of the cells. The measurement duct was designed and built to allow for real-time calculation of mass flow rate, temperature, static pressure, and combustion products using ISO standard 5167. Two measurement devices, each with their own pump to draw in a sample of gas through the air stream, determined oxygen, CO_2 and CO concentrations. A HEPA filter and a cold trap filtered out particulates before concentration measurements. The flow through the measurement duct for the test used in the model was 1.99 m^3/min. The HAR that was used in the model was determined with oxygen consumption calorimetry, which used an energy release of 13.1 MJ/kg of O_2 consumed. More information on the development of the test cell, and oxygen consumption calorimetry measurements can be found in work performed by Easton et al. [18].

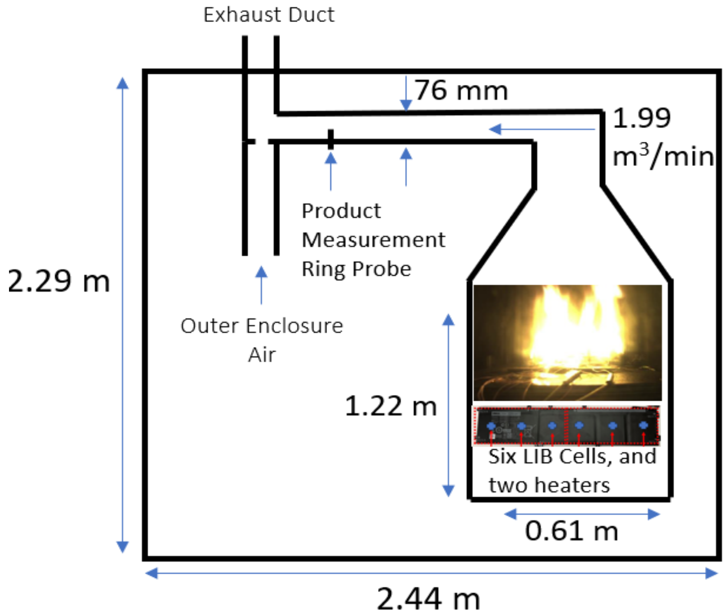

Figure 3. Lithium-ion battery experimental schematic.

III. Modeling

A previously developed model of the Cygnus vehicle during the Saffire burn events was used to predict the effect of a fire inside a spacecraft. This model uses Fire Dynamics Simulator (FDS), which is a large-eddy turbulent code developed by the National Institute of Standards and Technology (NIST) [19]. Placement of cargo were discussed in previous work [13]. Table 1 gives the initial atmospheric conditions for all models, as well as the flow boundary conditions.

For the validated Saffire model, the HAR and MGR were calculated from the SFU inlet and outlet temperature and CO_2 concentration experimental data, respectively [13]. The HCl MGR was also determined from experimental data. The LIB HAR was determined from oxygen consumption calorimetry [18]. The CO_2 MGR for LIB tests was calculated from CO_2 measurements in the measurement duct, but is not the focus of this paper. These values in the various simulations are applied to the outlet of the SFU, which is a thermally inert object that intakes cool cabin air and outputs combustion products and hot air. Figure 4 gives a schematic of how the HAR and MGR are applied to the SFU and input heat and combustion products into Cygnus. The graphs in Figure 4 represent the HAR and MGR that are used in the LIB simulations. No combustion or flame properties were used in the model. The same convective heat transfer coefficient of 150 W/m^2-K that was calibrated to experimental data in previous work was applied to the surfaces of the cargo in these simulations [15].

Table 1. Atmospheric initial conditions and flow boundary conditions.

Pressure (Pa)	5.42×10^4
Volume (m^3)	16.2
Density (kg/m^3)	0.639
Temperature (K)	297.5
CO_2 (ppm)	5381
O_2 (%)	30.9
Vehicle ECLSS (m^3/min)	3.72
Saffire Flow Duct (m^3/min)	1.68
Saffire Avionics (m^3/min)	0.78
FFD (m^3/min)	1.02

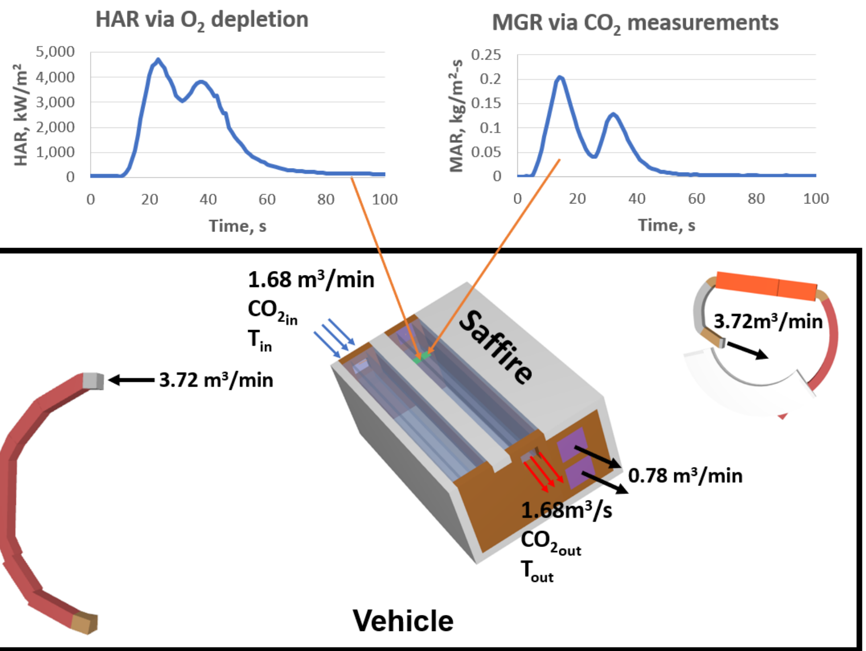

Figure 4. Cygnus vehicle model schematic highlighting implementation of MGR and HAR for the LIB fire predictions.

The first set of simulations focused on HCl transport in the vehicle. Since the SIBAL burn event in Saffire VI also released a bottle of HCl, concentration data was available in the FFD to compare to the simulation. The Saffire VI SIBAL simulations from previous work was re-simulated after adding the MGR of HCl from the SFU into Cygnus and applying the uptake rate at the cargo. The MGR of HCl into Cygnus from the SFU was $2.68x10^{-3}$ kg/m^2-s applied to a 5 cm x 5 cm surface area for 90s. Integrating this gave a total mass of HCl of 0.59 g, which matched the calculated amount in the bottle, as well as the steady state value of the HCl concentration in a simulation that did not have any surface adsorption imposed. Tests were executed on anodized aluminum surfaces at 50% humidity as described in section II and were shown to have an approximate rate of uptake given by Eq. 1: [17]

$$\dot{R} = 3.32x10^{-3}[HCl]\ kg/m^2 - s \tag{1}$$

where [HCl] is the mass fraction of HCl. This uptake rate of HCl was applied to the tan cargo bags in Cygnus, as demonstrated by Figure 5 which provides two contours of HCl in the forward port standoff. It was also assumed that any HCl that made its way into the ECLSS was fully adsorbed.

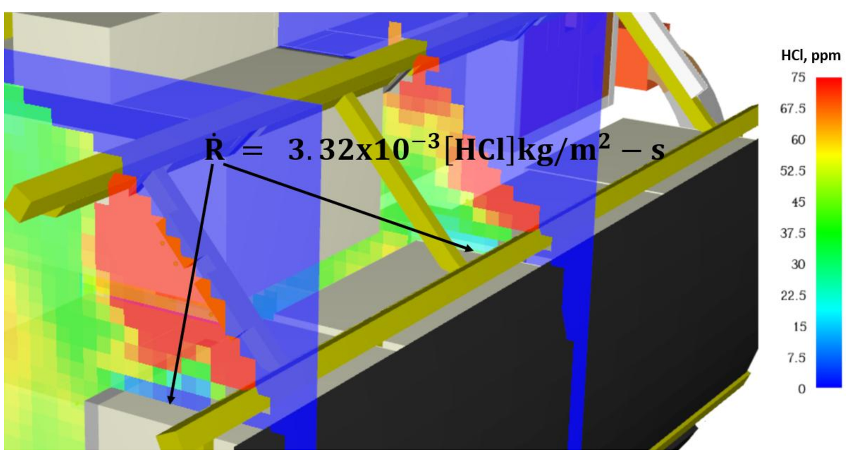

Figure 5. Example HCl contours highlighting the tan cargo surfaces the HCl uptake rate is applied.

A strategy for extinguishing a fire in an enclosed pressure vessel in a microgravity environment is to turn off the flow in a vehicle in order to starve the fire of oxygen. While this can be effective, stagnation of flow can lead to pockets of high concentration of hazardous combustion products. A simulation was run in which the ECLSS, SFU, and avionics flow were turned off once the FFD reached the 1-hour Spacecraft Maximum Allowable Concentration (SMAC) [20] of HCl, which was approximately 90 s for this simulation. A subsequent simulation turned the flow back on once the temperature returned to initial values.

The last set of simulations focused on the effect that the increased HAR provided by the LIB had on the vehicle. The temperature at the RS locations for the LIB simulation are compared to the temperatures of the Saffire VI SIBAL burn event. Additional simulations were completed that assigned material thermal properties to the cargo to see if the surfaces became hot enough to become hazardous.

IV. Results and Discussion

The concentration of HCl from the bottle release in Saffire VI SIBAL at the FFD is shown in Figure 6 against the model prediction. The peak concentration of 32 ppm and time to peak of 100 s match well with experimental results. This indicates that the bulk cabin flow and the release of the HCl bottle from the SFU in the simulation match the experiment. The drop in concentration happened significantly faster in the experiment than in the model. There are a couple reasons this discrepancy might exist. First, there was a lot of surface area in the FFD, as well as losses from the combustion product monitor that are not accounted for in the model which could add further decay. This is similar to the explanation of lower temperature in the FFD experiments compared to simulations during previous model development [10]. Second, the heat transfer coefficient that was calibrated during previous model development [11] is representative of an effective heat transfer coefficient to account for surfaces that are not perfectly rectangular or smooth, but amorphous, rough, and porous, hence underestimating the real surface area participating in heat transfer, and likely mass transfer. This increased surface area, as well as mixed materials of the surface would lend itself to the same type of calibration of an effective uptake rate as the effective heat transfer coefficient if a more accurate prediction is needed. For this work, the simulation compares well enough with experimental data that it can be used to explore the effect of flow on the fate of acid gas.

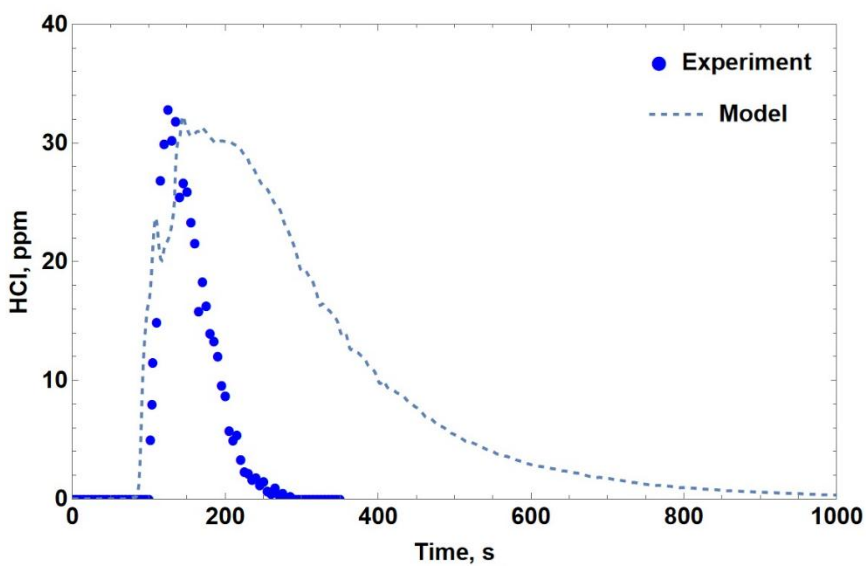

Figure 6. Prediction of HCl concentration at FFD against experiment during Saffire VI SIBAL burn.

Next, the ECLSS, as well as the SFU and avionics flow in Saffire were turned off when the FFD reached 5ppm, which is the 1 hour SMAC for HCl. This event was triggered in the simulation at 90 s. With the flow turned off, the concentration reached above 50 ppm and fell much slower. Figure 7 shows the original prediction against the prediction where the flow is shut off. The next simulation turned all the flow systems back on after the temperature in the cabin reached its initial value, which was at 410 s. The concentration at the FFD immediately began to fall at an accelerated rate, indicating the importance of flow for the removal of hazardous products from the atmosphere. This could further be demonstrated by the mass of HCl in the domain across the three simulations, which is provided by

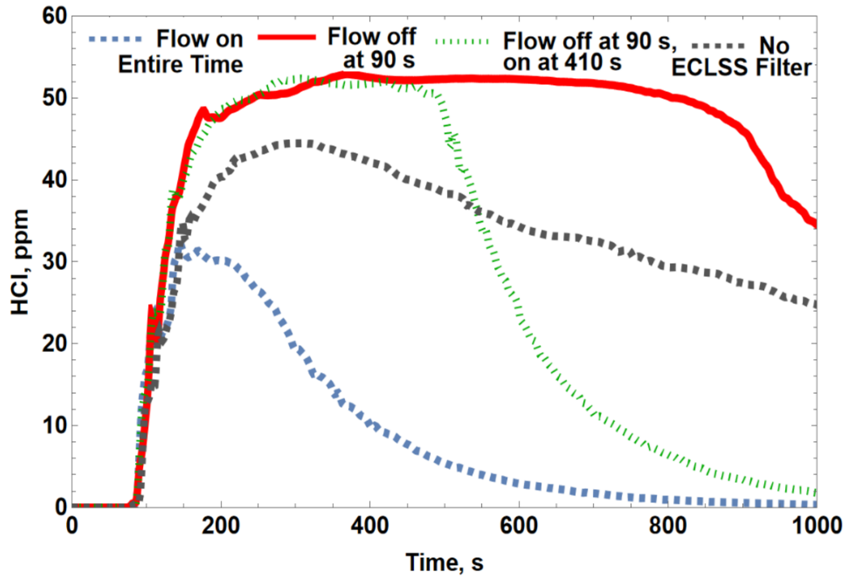

Figure 7. Prediction of HCl concentration at FFD with various settings of the ECLSS system.

Figure 8. An additional simulation was performed to highlight the ECLSS's contribution to the HCl decay from the atmosphere, which is shown in gray in Figure 7. This proves to be a significant contribution and additional experimental HCl sensors at the outlet of the ECLSS would be needed to validate the assumption.

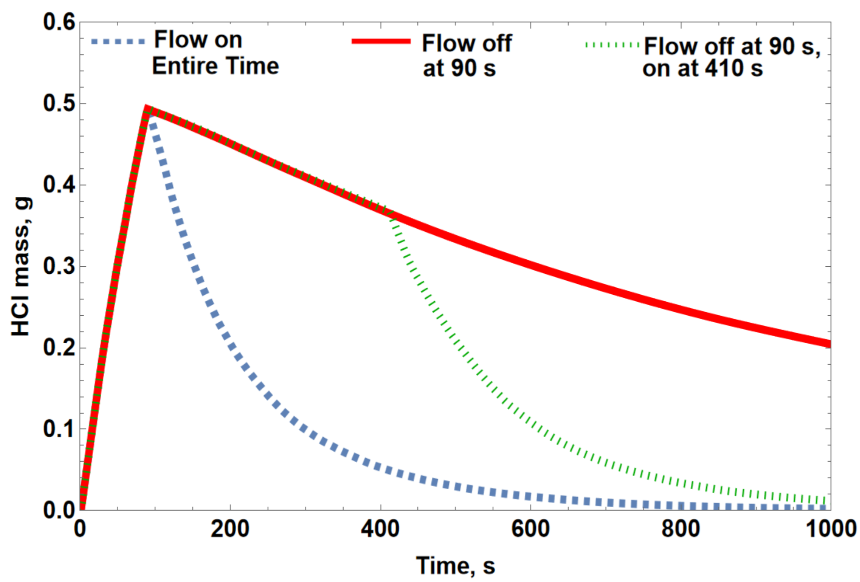

Figure 8. Total HCl mass in domain of model.

Figure 9 and Figure 10 show the response of RS3 and RS6, respectively for the three simulations. Concentration reached approximately 160 ppm at RS3 and 120 ppm for RS6. For RS3, HCl returned to effectively 0 by 1000 s, compared to RS6 where the concentration was still decreasing in the case where the flow was shut off. RS3 is in a standoff where the volume to surface area was much higher, allowing for more uptake and hence more removal of HCl from the atmosphere. RS6 was located in a more open area, away from surfaces that uptake HCl. In that case, the HCl stayed in the atmosphere surrounding RS6 until the flow is turned back on.

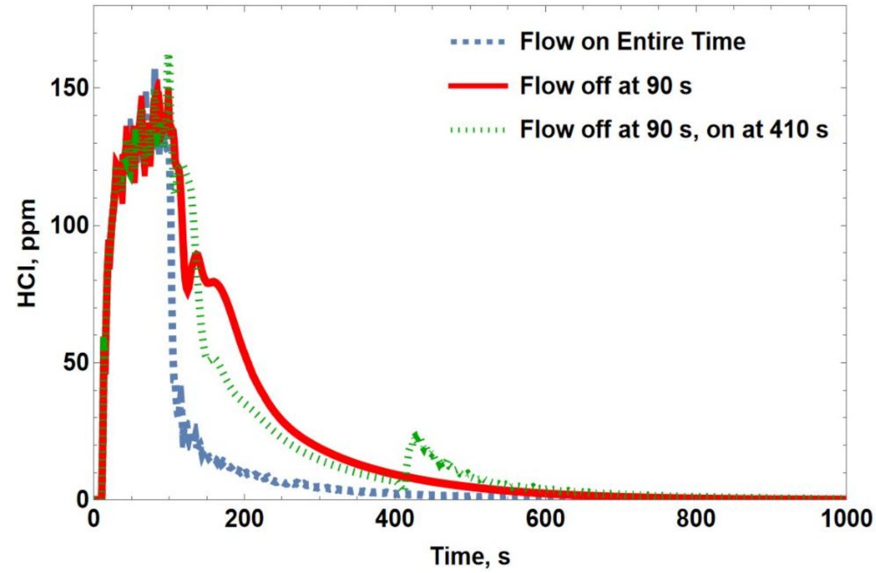

Figure 9. Prediction of HCl concentration at RS3 with various settings of the ECLSS system.

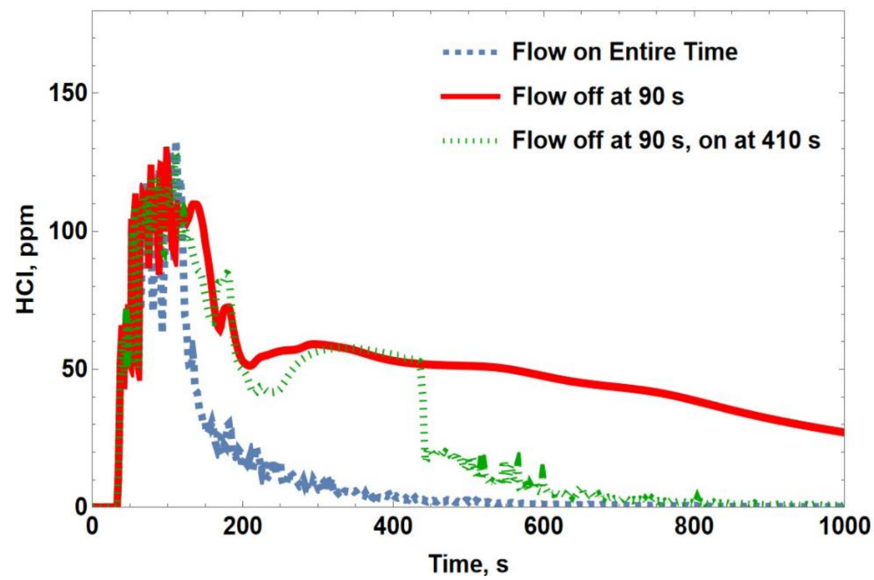

Figure 10. Prediction of HCl concentration at RS6 with various settings of the ECLSS system.

The next set of simulations used the HAR of the LIB cell pack test in place of the HAR from the SIBAL test in Saffire VI. The HAR is derived from ground based (1-g testing) and applied as an input in a 0-g model. Despite not having 0-g data of a LIB fire and the differences that it would provide in the HAR curve (fire growth, entrainment, heat transfer, etc.), this still provides a good prediction of a fire with an order of magnitude more peak and total energy compared to the Saffire material burn events. The max heat release rate for the battery was 23.63 kW, compared to 0.45 kW for the SIBAL burn. The total heat addition into the domain was 798 kJ vs. 124 kJ. Similar to the SIBAL test, the two remote sensors in the main flow path of Saffire (RS3 and RS6) produced the most noticeable temperature response, with RS2, RS4, and RS5 providing negligible response. RS1, which was near the ECLSS outlet on the nadir side of the vehicle, saw a brief 1 °C increase in the LIB case, compared to negligible response for the SIBAL case.

Figure 11 shows the temperature at the exhaust of the SFU for the LIB case. The SFU outlet reached over 450 °C in the LIB simulation and returned to baseline at around 100 s. This is consistent with the profile of the HAR presented in Figure 4, as is expected with the surfaces of the SFU being adiabatic. The HAR for the SIBAL case was determined to effectively match the exhaust temperature of the SFU. This is why even though the flame spread ended at 140 s,

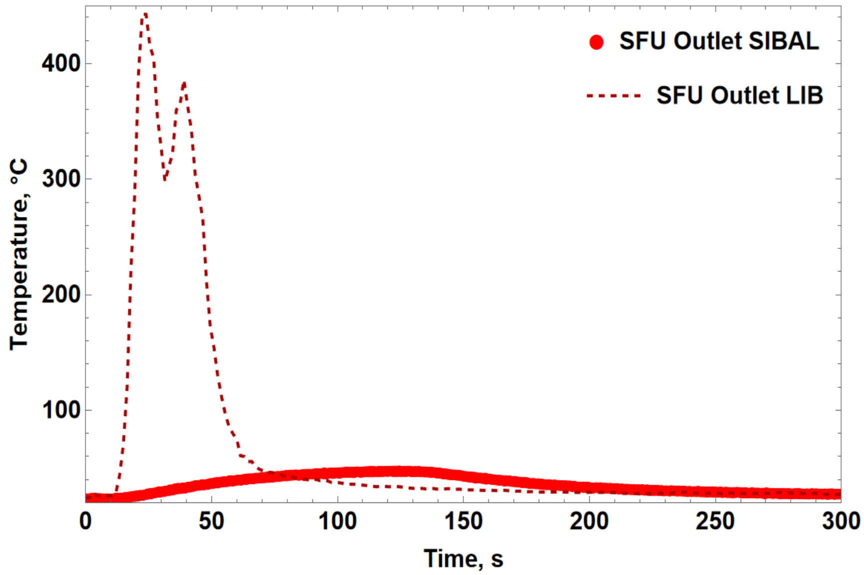

Figure 11. Prediction of temperature at the SFU exhaust for LIB simulation, compared to SFU exhaust temperature for SIBAL case.

heat is still transported into the cabin from the SFU. The HAR effectively included all the heat from the combustion of SIBAL and the heat from the surfaces that were released into the cabin.

Figures 12 and 13 give the temperature prediction for the LIB against the Saffire SIBAL case at RS3 and RS6, respectively. While the increase in temperature for the SIBAL case was no more than 3 degrees, significant temperature increase could be seen in the LIB case. This increased atmospheric temperature poses a hazard to the crew both externally via skin burn and internally via the inhalation of high temperature gas [21].

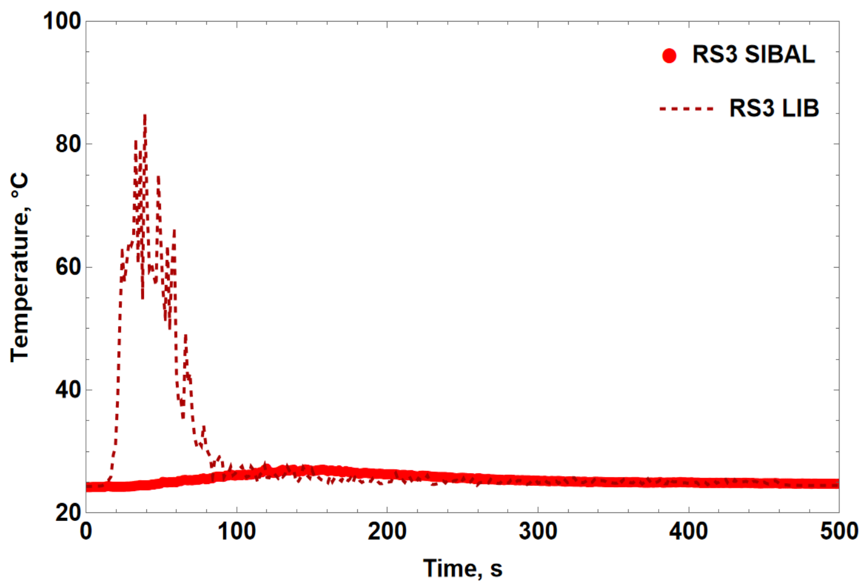

Figure 12. Prediction of temperature at RS3 for LIB against Saffire VI SIBAL case.

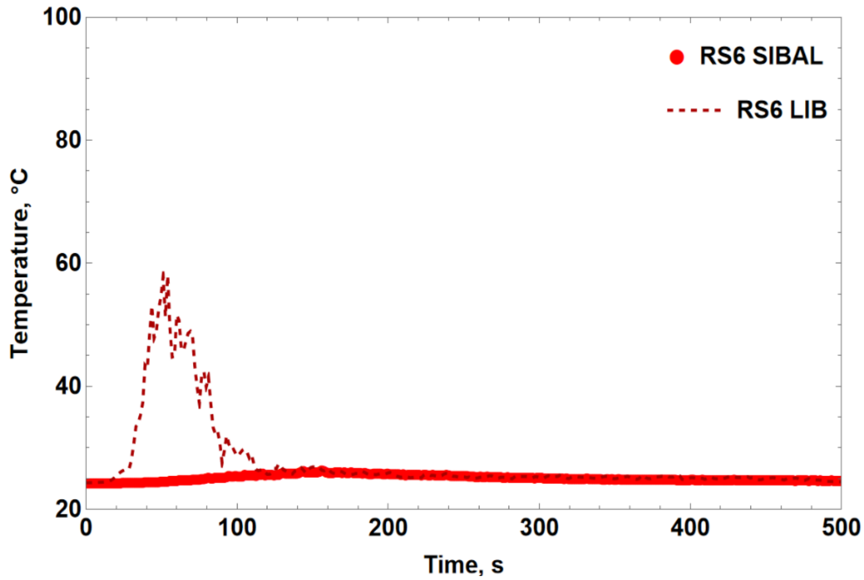

Figure 13. Prediction of temperature at RS6 for LIB against Saffire VI SIBAL case.

To explore additional hazards in regard to increased surface temperature, additional simulations were run where surface thermal properties were also assigned to cargo in the channels. Steel and aluminum were first chosen as realistic metals, despite the bags of trash and cargo likely having multiple materials. Table 2 shows the material properties used. Figure 14 shows the surface temperature at the surface directly below RS3. In comparing the two metals, the increased thermal diffusivity of the aluminum transported heat away from the surface and into the cool center, while heat stayed longer at the surface of the steel. The increased thermal mass of the steel corresponds to a lower steady state temperature. In any case, the temperature did not reach above 0.5 °C of the initial temperature, showing that surface temperature was not likely to be a critical hazard to the crew beyond surfaces directly in contact with a flame. This is also an indication that using an isothermal boundary condition at surfaces will in most cases provide a good prediction of the conditions of the atmosphere inside the vehicle.

The material was then changed to foam to demonstrate how hot a material with a much lower thermal mass could become. Foam is present in Cygnus, as well as being an available material in the Pyrosim library. The surface reached 45 °C but returned to its initial temperature by 200 s. Surface temperatures reaching 60 °C, as cited by ASTM standard C1055-03 [22], are often deemed hazardous. While the amount of heat added to the vehicle in these simulations did not produce surfaces hot enough to be hazardous, tests are planned to burn entire laptops and multiple battery packs. These tests could produce a larger and more sustained burn event, in which case the surface temperature could become a risk factor.

Table 2. Solid surface thermal properties.

	Aluminum	Steel	Foam
k (W/m-K)	237	45.8	0.05
C_p (J/kg-K)	900	460	1700
ρ (kg/m^3)	2700	7850	28
α (m^2/s)	9.75×10^{-5}	1.3×10^{-5}	1.05×10^{-6}

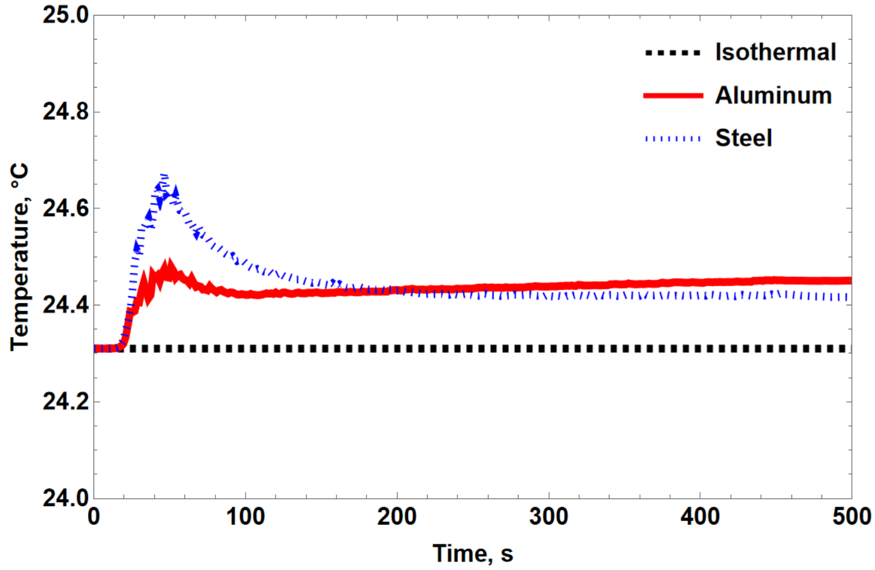

Figure 14. Surface temperature prediction during LIB simulation at cargo below RS3.

V. Conclusions

A previously validated model of the Cygnus vehicle during the burn events of the Saffire experimental campaign was used to simulate other fire scenarios of interest. First, an HCl MGR was added to the Saffire VI SIBAL model that was provided experimentally and an HCl uptake rate that was experimentally measured was implemented at the cargo of the vehicle. The simulated prediction of the HCl at the FFD matched the peak of the experimental data, with some deviations at the tail end of the response. Next, the flow in the vehicle was turned off once HCl reached 5 ppm at the FFD, which greatly reduced the rate of uptake and left high concentrations of HCl in the vehicle for extended periods of time. An additional simulation where the flow was turned back on after the temperature returned to baseline showed that the rate of uptake of HCl returned to the previous rate. The next set of simulations focused on the heat transfer from a LIB fire, and the results were compared to the previous SIBAL simulation. As expected, the increased HAR provided by the LIB produced higher temperatures for the remote sensors that were in the flow path of Saffire. Simulations where the material were changed from isothermal to either steel or aluminum and measured the surface temperature of the cargo provided an insignificant difference. Future experiments could provide heat and product release of multicell LIBs with entire laptops and battery fire bags burned that would provide even larger heat release for a sustained time. The burning of these LIBs, as well as other electronics, will create other acid gases that will need to be further investigated to determine their fate in a spacecraft.

Acknowledgments

The Saffire project was supported by NASA's Advanced Exploration Systems Division. The authors would like to thank the international Saffire science team, with various agencies that include ESA, JAXA, CNES, RSA, DLR, the Russian Academy of Sciences and NASA. The authors are grateful for the efforts of ZIN Technologies, NG, and the on-orbit crew of the ISS on the Saffire project, as well as Ryan Briggs and Mathieu Fradet from JPL for CPM development and testing.

References

[1] Fortenberry, C., and Meyer, M., "Smoke Aerosol Experiments for the Next Generation of Space Vehicles," in *54th International Conference on Environmental Systems,* Prague, Czechia, ICES-2025-551, 2025.

[2] NASA Exploration Atmospheres Working Group, "Recommendations for exploration spacecraft internal atmospheres: The final report of the NASA exploration atmospheres working group," NASA/TP-2010-216134, NASA, 2010.

[3] J., Norcross, P., Norsk, J., Law, D., Arias, J., Conkin, M., Perchonok, A., Menon, J., Huff, J., Fogarty, J. H., and Wessel, S., Whitmire, "Effects of the 8 psia / 32% O2 Atmosphere on the Human in the Spaceflight Environment," NASA/TM-2013-217377, 2013.

[4] R. W., Bricker, J. P., Crabb, and I. K., Spiker, "Apollo Command Module and Lunar Module Mockup Flammability Tests," NASA TN D-5654, 1970.

[5] R., Friedman, "Fire safety concerns in space operations," NASA TM 89848, 1987.

[6] J. H., Kimzey, "Skylab experiment M479 zero gravity flammability," *Skylab Results, Proc. Third Space Processing Symp.* Vol. 1, pp. 115-130, 1974.

[7] D., Urban, G., Ruff, P., Ferkul, J., Owens, S., Olson, M., Meyer, C., Fortenberry, J., Brooker, J., M., Graf, F., Casteel, G., Jomaas, B., Toth, C., Eigenbrod, J., T'ien, Y.-T., Liao, C., Fernandez-Pello, F., Meyer, G., Legros, A., Guibaud, N., Smirnov, and O., Fujita, "Fire Safety Implications of Preliminary Results from Saffire IV and V Experiments on Large Scale Spacecraft Fires," in *50th International Conference on Environmental Systems*, ICES-2021-266, 2021.

[8] G., Jomaas, J. T., Torero, C., Eigenbrod, J., Niehaus, S. L., Olson, P. V., Ferkul, G., Legros, C., Fernandez-Pello, A. J., Cowlard, S., Rouvreau, N., Smirnov, O., Fujita, J. S., T'ien, G. A., Ruff, and D. L., Urban, "Fire Safety in Space – Beyond Flammability Testing of Small Sample," *Acta Astronautica*, Vol. 109, pp. 208-216, 2015.

[9] D. L., Urban, G. A., Ruff, P., Ferkul, J., Easton, M., Johnston, J., Owens, J., S., Olson, C., Fortenberry, G., Graf, O., George, B., Toth, F., Meyer, C., Eigenbrod, J., S., T'ien, Y.-T., Liao, C., Fernandez-Pello, G., Legros, A., Guibaud, N. Smirnov, O., Fujita, U. R., Rojas, and G., Jomaas, "Preliminary Results from the Saffire VI Experiment," in *53rd International Conference on Environmental Systems*, Louisville, KY, ICES-2024-365, 2024.

[10] J., Brooker, and J., Niehaus, "Model Development of Large-Scale Spacecraft Fires during the Saffire-IV Experiments," in *51st International Conference on Environmental Systems*, Minneapolis, MN, ICES-2022-278, 2022.

[11] J., Niehaus, and J., Brooker, "Vehicle Modeling during the Burning of Cotton Samples in the Saffire IV and V Experiments," in *52nd International Conference on Environmental Systems*, Calgary, Canada, ICES-2023-204, 2023.

[12] J., Niehaus, J., Brooker, D., Urban, and G., Ruff, "Vehicle Modeling during the Burning of Thermally Thick Samples in the Saffire V Experiments," in *53rd International Conference on Environmental Systems*, Louisville, KY, ICES-2024-310, 2024.

[13] J., Niehaus, J., Brooker, D., Urban, and G., Ruff, "Vehicle Modeling During the Burn Events in the Saffire VI Experiments," in *54th International Conference on Environmental Systems,* Prague, Czechia, ICES-2025-156, 2025.

[14] J., Niehaus, S., Gokoglu, S., Mazumder, G., Berger, and J., Easton, "Modeling hydrogen chloride and aluminum surface interactions for spacecraft fire safety applications," *Journal of Spacecraft and Rockets* vol. 57, no. 2, pp. 217-224, 2020.

[15] J. E., Niehaus, and S., Mazumder, "Multiscale Model for Hydrogen Chloride Uptake on Aluminum for Spacecraft Fire Safety," *Journal of Spacecraft and Rockets*, vol. 61, no. 3, pp. 839-846, 2024.

[16] B., Tobias, and C., McMillan, C., "Evolution of Hardware and Philosophy of Emergency Response Actions on the International Space Station and Future Spacecrafts," in *17th International Conference on Space Operations*, Dubai, United Arab Emirates, SpaceOps- 2020, ID # 187, 2023.

[17] J., Niehaus, S., Gokoglu, S., Mazumder, G., Berger, and J., Easton, "Effect of Humidity on Surface Interaction of Gaseous HCl and Aluminum for Spacecraft Fire Safety Applications," in *International Conference on Environmental Systems*, ICES-2020-341, 2020.

[18] J., Easton, Y.-T., Liao, R., Padilla, G., Berger, J., Owens, C., Fortenberry, D., Urban, D., Dietrich, T., Miller, and T., DeMichael, "Measurement of Heat Release Rate, Aerosol, and Gas Products During Lithium-Ion Battery Thermal Runaway in Devices." in *54th International Conference on Environmental Systems*, Prague, Czechia, ICES-2025-426, 2025.

[19] Pyrosim, Software Package, Ver. 2021-2, Thunderhead Engineering, Manhattan, KS, 2014.

[20] J. T., James, "Spacecraft maximum allowable concentrations for airborne contaminants," No. JSC-CN-18135, 2008.

[21] Y.-G., Lva, J., Liua, and J., Zhang, "Theoretical evaluation of burns to the human respiratory tract due to inhalation of hot gas in the early stage of fires," *Burns*, vol. 32, no. 4, pp. 436-446, 2006.

[22]. American Society for Testing and Materials, "Standard guide for heated system surface conditions that produce contact burn injuries," ASTM C1055-03, 2009.